High-field, Hall-effect spectroscopy applied to n-type germanium

Larry D. Partain,* Mysore R. Lakshminarayana,† and Gerard J. Sullivan‡
Electrical Engineering Department, University of Delaware, Newark, Delaware 19711
and Francis Bitter National Magnet Laboratory, Massachusetts Institute of Technology, Cambridge, Massachusetts 02139
(Received 6 November 1978)

Hall-effect data measured at high-magnetic-field strengths as a function of temperature have been used to demonstrate a new method for determining the concentration and energy spacing from the band edge of impurities in semiconducting materials not previously measurable from Hall-type experiments. Applied to antimony-doped, n-type germanium, three deep levels have been identified with the following concentrations and energy spacings below the conduction-band edge: (1.00 ± 0.02) $(10^{12})/\text{cm}^3$ at 0.0590 ± 0.005 eV, $(1.37\pm0.02)(10^{12})/\text{cm}^3$ at 0.0977 ± 0.0005 eV, and (5.87 ± 0.02) $(10^{12})/\text{cm}^3$ at 0.199 ± 0.005 eV. The middle and deepest energies correspond to known Ag and Au levels, respectively. The shallowest value is newly reported here. The strong temperature dependence of the low-field, Hall-effect correction factors have been measured and shown to prevent similar analysis of low-magnetic-field data. A new criterion has been developed to explain the temperatures needed to ionize specific impurity levels.

I. INTRODUCTION

When Hall-effect measurements of carrier concentration are made on materials at the magnetic fields strengths B readily available (1–10 kG) in typical laboratories, the results are usually uncertain by an unknown correction factor.[1,2] At sufficiently high-field strengths, the value of this correction factor reduces to 1, and high-accuracy data are obtained for the difference between the conduction-electron and hole concentrations in semiconducting materials. A first-order criterion specifying the high-field region is to require that the squared product of mobility μ and magnetic field strength (in a consistent set of units such as B in Wb/m^2 and μ in $\text{m}^2/\text{V}-\text{sec}$) be much greater than 1. As an example, with a mobility of 1000 $\text{cm}^2/\text{V sec}$, this squared product would equal ten when B is 31.6 kG. In this paper, existing theory is extended to show how previously undetectable energy levels and densities of donors or acceptors can be identified from high-field, Hall-effect data taken as a function of temperature. For this a high-field value of 129.2 kG was used between liquid-nitrogen and room temperatures. A new criterion is defined to establish what temperatures are needed to ionize a given impurity level. Experimental data are presented on n-type germanium that identify three, deeper-lying donor levels, two of which correspond to known Au and Ag levels, and that demonstrate the prohibitively large uncertainty present in low B field results.

II. THEORY

In this section, existing theory is extended to justify the new approach to analyzing experimental data. For materials doped with donor and acceptor impurities, the concentrations of electrons n and holes p are determined by the densities of ionized donors N_D^I and ionized acceptors N_A^I so that[3]

$$n-p=N_D^I-N_A^I\,. \tag{1}$$

For r discrete donor levels of density N_{Di} and energy E_{Di} in the band gap E_G between the conduction- and valence-band edges E_c and E_v, respectively, and s acceptors of density N_{Aj} and energy E_{Aj} as shown in Fig. 1 as a function of electron energy E, the density of ionized impurities is obtained by summing the product of the levels' doping density times the probability the level is ionized. Using Fermi-Dirac statistics, one obtains[4]

$$N_D^I=\sum_{i=1}^{r}\frac{N_{Di}}{1+(1/\beta)\exp[-(E_{Di}-E_F)/KT]} \tag{2}$$

and

$$N_A^I=\sum_{j=1}^{s}\frac{N_{Aj}}{1+\beta\exp[E_{Aj}-E_F)/KT]}\,, \tag{3}$$

considering only the ground state (no excited states) of each impurity level. Here E_F is the Fermi energy, K is Boltzmann's constant, T is the absolute temperature, and β is equal to $\frac{1}{2}$. This β accounts for the localized nature of each impurity state and the resulting electrostatic repulsion which prevents two electrons from occupying the same impurity site even through permitted by the Pauli exclusion principle.[5] Restricting attention to materials doped lightly enough to use Maxwell-Boltzmann statistics, the conduction electron and hole concentrations are given by

$$n=A_n T^{3/2}e^{-(E_c-E_F)/KT} \tag{4}$$

and

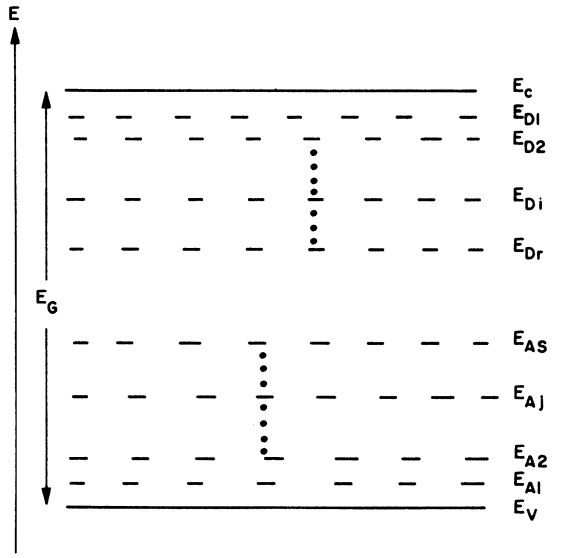

FIG. 1. Location of discrete donor levels E_{Di} and discrete acceptor levels E_{Aj} relative to the conduction and valence-band edges E_c and E_V, respectively.

$$p = A_p T^{3/2} e^{-(E_F - E_v)/KT}, \tag{5}$$

where

$$A_\alpha = 2(2m_\alpha^* K/h^2)^{3/2}, \tag{6}$$

with h being Planck's constant and m_α^* signifying the density of states effective mass for the conduction electrons m_n^*, the holes m_p^*, or the free electrons $m_0^* = m_0$. For materials with g equivalent, ellipsoidal valleys, one finds[6,7]

$$m_\alpha^* = g^{2/3}(m_x m_y m_z)^{1/3}, \tag{7}$$

where m_x, m_y, and m_z are the effective masses along each axis of the ellipsoid.

Next, the above existing theory is extended by solving Eq. (4) for E_F and substituting this into Eqs. (2), (3), and (5) to give Eq. (1) as

$$n = \sum_{i=1}^{r} n_i - \sum_{j=1}^{s} p_j + p, \tag{8}$$

where n_i and p_j are the concentrations, respectively, of ionized donors of level i and or ionized acceptors of level j given by

$$n_i = \frac{N_{Di}}{1 + n/(m_n^*/m_0)^{3/2} w(E_c - E_{Di}, T)}, \tag{9}$$

$$p_j = \frac{N_{Aj}}{1 + (m_n^*/m_0)^{3/2} w(E_c - E_{Aj}, T)/n}, \tag{10}$$

with

$$w(E_i, T) = \beta A_0 T^{3/2} e^{-E_i/KT} \tag{11}$$

and

$$p = \left(\frac{m_n^* m_p^*}{m_0 m_0}\right)^{3/2} \frac{w^2(-E_G/2, T)}{n}. \tag{12}$$

These new Eqs. (8)–(12) completely specify the conduction-electron concentration as a function of temperature in terms of the impurity levels and their density, the band gap, and the density of states effective mass. An analagous expression for p is obtained by solving Eq. (5) for E_F followed by similar substitutions. Of course p can be obtained once n is known from the well-known result

$$np = A_n A_p T^3 e^{-E_G/KT} \tag{13}$$

specified by Eqs. (4) and (5).

For cases where E_F is many KT above the highest acceptor level E_{As}, Eq. (3) shows that N_A^I is well approximated by

$$N_A^I \simeq \sum_{j=1}^{s} N_{Aj}. \tag{14}$$

If in addition $n \gg p$, then Eq. (8) is well approximated by

$$n \simeq \sum_{i=1}^{r} \frac{N_{Di}}{1 + n/(m_n^*/m_0)^{3/2} w(E_c - E_{Di}, T)} - \sum_{j=1}^{s} N_{Aj}. \tag{15}$$

If one further assumes wide spacing between the donor levels so that when

$$E_F \simeq E_{D\alpha},$$

$$E_{D(\alpha+1)} - E_F \gg KT$$

and

$$E_F - E_{D(\alpha-1)} \gg KT,$$

then the above is further simplified to

$$n \simeq \frac{N_{D\alpha}}{1 + n/(m_n^*/m_0)^{3/2} w(E_c - E_{D\alpha}, T)} + \sum_{i=1}^{\alpha-1} N_{Di} - \sum_{j=1}^{s} N_{Aj}. \tag{16}$$

Rearranging terms in the above, substituting Eq. (11) for w, and taking the logarithm allows one to define a term F as

$$\ln F = \ln\left(\frac{n\left(n - \sum_{i=1}^{\alpha-1} N_{Di} + \sum_{j=1}^{s} N_{Aj}\right)}{\left(N_{D\alpha} + \sum_{i=1}^{\alpha-1} N_{Di} - \sum_{j=1}^{s} N_{Aj} - n\right) T^{3/2}}\right) = \ln(\beta A_n) - (E_c - E_{D\alpha})/KT. \tag{17}$$

For E_F many KT below the lowest donor level with $p \gg n$ and the acceptor levels spaced sufficiently far apart in energy, an expression in p analogous to Eq. (17), but involving A_p and $E_{A\alpha} - E_v$, is obtained. At low enough temperature, only the shal-

lowest donor is involved and Eq. (17) can be written in its low-temperature form as

$$\ln F_{LT} = \ln\left(\frac{n\left(n+\sum_{j=1}^{s} N_{Aj}\right)}{\left(N_{D1}-\sum_{j=1}^{s} N_{Aj}-n\right)T^{3/2}}\right)$$

$$= \ln(\beta A_n) - (E_c - E_{D1})/KT\,. \qquad (18)$$

At T approaches absolute zero, the impurity ionization, and thus n approach zero. Then if the total density of acceptors is non-negligible so that $n \ll \sum_{j=1}^{s} N_{Aj}$, Eq. (18) shows that

$$\ln n - \tfrac{3}{2}\ln T = \ln\left(\frac{N_{D1}-\sum_{j=1}^{s} N_{Aj}}{\sum_{j=1}^{s} N_{Aj}}\right) + \ln(\beta A_n) - (E_c - E_{D1})/KT\,, \qquad (19)$$

where the $\frac{3}{2}\ln T$ term is small at low T. However, if there are no acceptors, Eq. (18) simplifies at low temperature to

$$\ln n - \tfrac{3}{4}\ln T = \tfrac{1}{2}\ln N_{D1} + \tfrac{1}{2}\ln(\beta A_n) - (E_c - E_{D1})/2KT\,. \qquad (20)$$

The terms in the two equations above have been rearranged to more clearly indicate the relation of of a low-temperature $\ln n$ vs $1/T$ plot to the position of the shallowest donor level below the conduction-band edge. Particularly note here the uncertainty by a factor of 2 in the values of energy levels determined by low-temperature $\ln n$ vs $1/T$ plots if it is not known whether or not the material is compensated.

From Eq. (18), a low-temperature plot of $\ln F_{LT}$ vs $1/T$ should give a straight line graph with a negative slope of $(E_c - E_{D1})/K$ and with an intercept determined by the density of states effective mass, provided that the two fitting parameters N_{D1} and $\sum_{j=1}^{s} N_{Aj}$ are chosen correctly. Incorrect choice gives an incorrect intercept or makes the data points lie along a curved rather than a straight line. If the levels are spaced sufficiently far apart in energy, higher levels should be identified by $\ln F$ vs $1/T$ plots of Eq. (17) with the same intercept and a single new fitting parameter $N_{D\alpha}$ as each deeper level is excited in turn. The modifications of this treatment to treat acceptors in p-type material should be obvious. The temperatures needed to ionize a given impurity level can be determined from plots of $w(E_c - E_D, T)$ vs $KT/(E_c - E_D)$, as shown in Fig. 2. When $w(E_D - E_{D\alpha}, T)$ is ten times larger than $n/(m_n^*/m_0)^{3/2}$, the denominator of Eq. (9) equals 1.1 so that the energy level $E_{D\alpha}$ is 90% ionized. When it is 100 times larger, this level is 99% ionized and so on. With an n of about $10^{14}/\text{cm}^3$ and $E_c - E_{D\alpha} = 0.020$ eV and a reasonable effectiveness ratio m_n^*/m_0 on the order on one, KT need only be about 0.2 $(E_c - E_{D\alpha})$ to ionize 99% of the donor sites at this level according to Fig. 2 and Eq. (9).

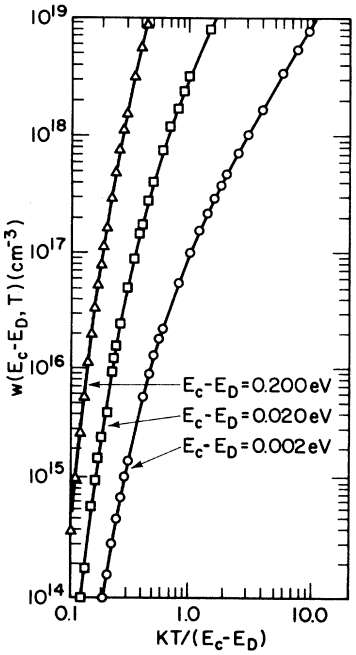

FIG. 2. Plot of $w(E_c - E_D, T)$ as a function of $KT/(E_c - E_D)$ for three values of $E_c - E_D$.

Thus at lower carrier concentrations, KT values well below the depth of the level below the band edge can provide almost total ionization. This arises in the following way. When a donor level E_D is located many KT below the band edge E_c, only a small fraction of the very numerous conduction-band states are accessible. However, if the doping concentration is low, this accessible fraction of band states can be larger than the doping concentration. Since a basic assumption of thermodynamics is that occupation of all *accessible* states is equally likely,[5] more conduction-band states would be occupied on the average by electrons than the donor states. At higher doping concentrations this is not true and higher temperatures must be used to make even larger numbers of the conduction band states accessible before a level is mostly ionized. This is described quantitatively by the curves of Fig. 2 where KT must become larger compared to $E_c - E_D$ (for a given $E_c - E_D$ value) as the donor concentration is increased so that w, for example, remains 100 times larger than $n \simeq N_D$ to

provide 99% ionization of the level [as specified by Eq. (9)]. The above is a convenient way of determining the degree of ionization of a level and is new to the best of our knowledge.

III. EXPERIMENTAL RESULTS AND ANALYSIS

Hall-effect measurements were made on antimony-doped, n-type germanium samples of rectangular parallelepiped shape with approximate dimensions of 1-cm length (in the direction of current), 0.2-cm height (in the direction of Hall voltage), and 0.1-cm width (in the magnetic field direction). X-ray diffraction was used to crystallographically orient the samples to within ±1 degree so that the B field was in the [001] direction, the current was in the [100] direction, and the Hall field was in the [010] direction. Small-dot Ohmic contacts were obtained by alloying tin-lead–antimony solder to the samples in a standard five-point, Hall-effect configuration.[2] The magnetic field was produced in a solenoidal Bitter magnet. The high magnetic field strangths of 129.2 kG, constant within ±0.1%, were provided with current from the 10 MW power supplies of the Francis Bitter National Magnet Laboratory at M.I.T. The low fields of 0.5 kG magnitude were provided by a 100 A dc power supply of similar stability. Temperature control was obtained to within ±½ K by an electrically heated cold finger surrounded by a metal vacuum jacket that was inserted into liquid nitrogen. Temperature values to within ±½ K were measured with a platinum resistance thermometers imbedded in the heat sink on which the samples were mounted.

Values for the differences between the conduction-electron and hole concentrations were determined from the reciprocal of the Hall coefficient using $1/R_H q$, where q is the electronic charge. The results obtained at the high B field ($1/R_\infty q$) are shown by the square data points at the bottom of Fig. 3 as a function of one over the temperature for values between 77 and 273 K. The estimated ±0.2% accuracy of these data is indicated by the physical size of the data points. The corresponding low-field values ($1/R_0 q$) are given by the circular data points at the top of this figure. The estimated ±1.0% accuracy of this noisier low-field data is indicated by the error bar.

At low enough fields $1/R_H q$ takes on its low-field limiting value specified by

$$1/R_0 q = (p-n)/AS\,, \tag{21}$$

where A and S are correction factors termed the anisotropy factor and the scattering ratio.[1,2] When the magnetic field is large enough to make $\mu^2 B^2 \gg 1$, the Hall coefficient directly gives

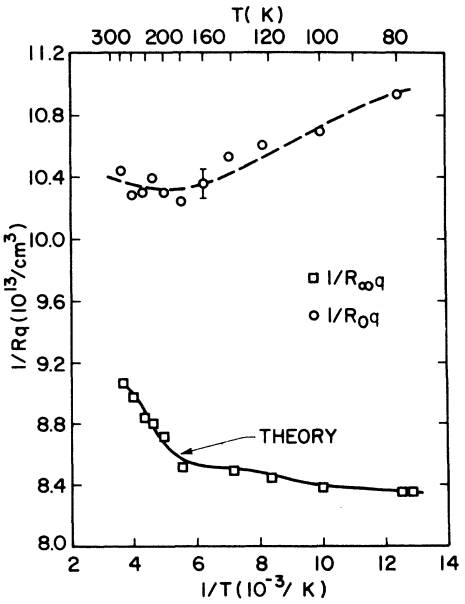

FIG. 3. Plots of experimental values of $1/R_0 q$ and theoretical and experimental values of $1/R_\infty q$ as a function of $1/T$.

$$1/R_\infty q = p - n\,, \tag{22}$$

unencumbered by correction terms. The measured low B field values of the conductivity mobility μ_σ and the Hall mobility μ_H as a function of $1/T$ are given by the data points in Fig. 4. Note that these differently defined[1,7] mobilities are on the same order of magnitude so that use of either gives similar estimates of the $\mu^2 B^2$ magnitude.[1,2] In par-

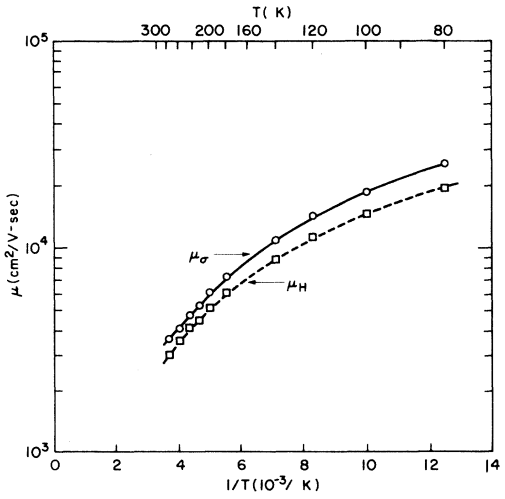

FIG. 4. Experimentally determined values of conductivity mobility μ_σ and Hall mobility μ_H as a function of $1/T$.

ticular note that for $B=129.2$ kG, the μ^2B^2 product was always greater than 14. Thus the high-field values of $1/R_\infty q$ in Fig. 3 give the true carrier concentration difference as a function of temperature. Note that μ^2B^2 is always less than 0.02 for the low-field data (where $B=0.5$ kG) so that low-field $1/R_0q$ values were always obtained. Also notice that this low-field data in Fig. 3 falls with increasing temperature (decreasing $1/T$ values) even though the actual carrier concentration increases. This difference is caused by the strong temperature dependence of the correction factor AS plotted in Fig. 5. It was obtained by taking the ratio of the experimental data of Fig. 3.

Assuming that $p \ll n$, the high-field results of Fig. 3 were replotted as $\ln F$ vs $1/T$ as shown in Fig. 6. For the lowest temperature points, a straight line plot with the correct $1/T=0$ intercept was obtained when the values

$$N_{D2}=(1.00\pm0.02)(10^{12})/\text{cm}^3$$

and

$$N_{D1}-\sum_{j=1}^{s}N_{Aj}=(8.290\pm0.002)(10^{13})/\text{cm}^3$$

were used. The intercept was calculated from Eqs. (6), (7), and (17) using ellipsoidal effective-mass values of $m_x=1.59m_0$ and $m_y=m_z=0.0815m_0$ and four, equivalent ellipsoidal valleys[7,8] which gave $m_n^*=0.553m_0$. As might have been expected considering Eqs. (19) and (20), the intercepts and slopes of the $\ln F$ vs $1/T$ were quite sensitive to the value chosen for $N_{D1}-\sum_{j=1}^{s}N_{Aj}$. The higher temperature points were best fit with $N_{D3}=(1.37$

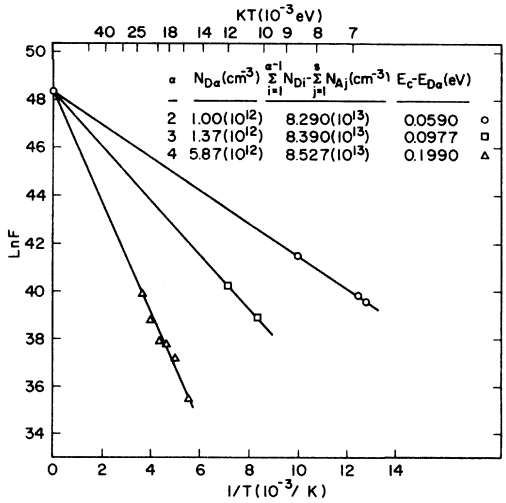

FIG. 6. Plots of $\ln F$ as a function of $1/T$ for the various values of $N_{D\alpha}$ and $\sum_{i=1}^{\alpha-1}N_{Di}-\sum_{j=1}^{s}N_{Aj}$ found to give a straight line fit to the experimental data.

$\pm0.02)(10^{12})/\text{cm}^3$ and $N_{D4}=(5.87\pm0.02)(10^{12})/\text{cm}^3$. The slopes gave energy levels of $E_c-E_{D2}=0.0590\pm0.0005$ eV, $E_c-E_{D3}=0.0977\pm0.0005$ eV, and $E_c-E_{D4}=0.199\pm0.0005$ eV. The error ranges were estimated from the experimental data scatter and the known accuracy of the measuring instruments. These parameter values and $E_G=0.67$ eV (See Ref. 7) were substituted into Eq. (8) which was solved as a transcendental equation by trial and error. Since only one term at a time on the right-hand side varied significantly with temper-

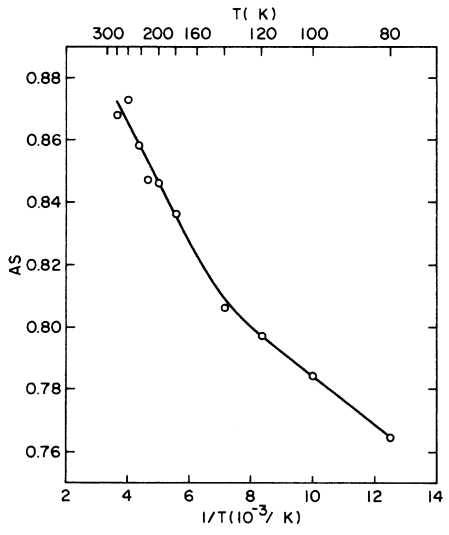

FIG. 5. Experimentally determined values of the correction factors AS as a function of $1/T$.

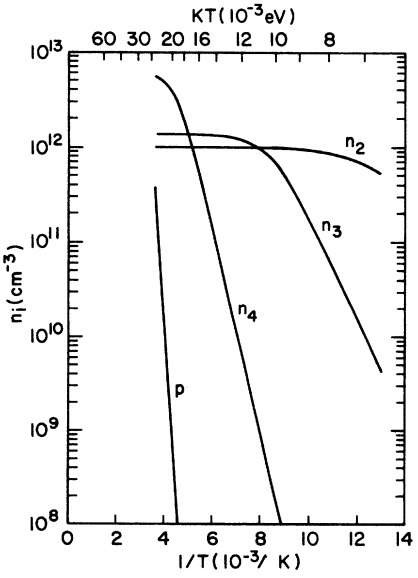

FIG. 7. Theoretical values of n_i and p as a function of $1/T$.

ature, such solutions were easily obtained. The results of this are shown as the solid line theoretical curve that fits the data points at the bottom of Fig. 3. This theoretical temperature dependence of each ionized donor level concentration n_i [see Eq. (8)] are shown in Fig. 7 along with the hole concentration p. As predicted by Fig. 2 for materials with n values of around $10^{14}/cm^3$, Figs. 6 and 7 indicate that each level is about 99% ionized at temperatures where KT is a few tenths of the depth of the donor level from the conduction-band edge. The near linear theoretical and experimental dependence of E_F on T was obtained by analyzing the theory and the measured square data points of Fig. 3 using Eq. (4) and is plotted in Fig. 8. The slight deviation from linearity is primarily due to the $T^{3/2}$ multiplying the exponential in Eq. (4). Comparison to known impurity levels in Ge shows that the measure values correspond approximately to an Au level at 0.20 eV and to an Ag level at 0.09 eV below the conduction-band edge.[9] To the best of our knowledge, the 0.059 eV level has not been previously reported.

At very low temperatures (liquid helium values approaching absolute zero), Geballe and Morin's data[10] shows that carriers begin to freeze out into the lowest donor level so that n varies over many orders of magnitude.[11] For this case the relatively small changes in AS such as shown in Fig. 5 are completely dominated by the huge variations in n. Thus accurate values for the shallowest donor level (which is 0.0097 ± 0.0002 eV for antimony doped germanium) can be obtained from $\ln n$ vs $1/T$ plots as demonstrated by Geballe and Morin[10] in their Fig. 1. The factor of 2 uncertainty [see Eqs. (19) and (20)] in energy level with such plots is removed by noting that these values were measured on highly compensated germanium (significant acceptor concentration present) which is evident by replotting their data as $\ln F$ vs $1/T$ (using the correction factor $AS = 0.8$ determined at liquid nitrogen temperature)[1] and noting that a straight line graph correctly intersecting the $1/T = 0$ axis as described by Eq. (17) is obtained with compensation on the order of $10^{13}/cm^3$.

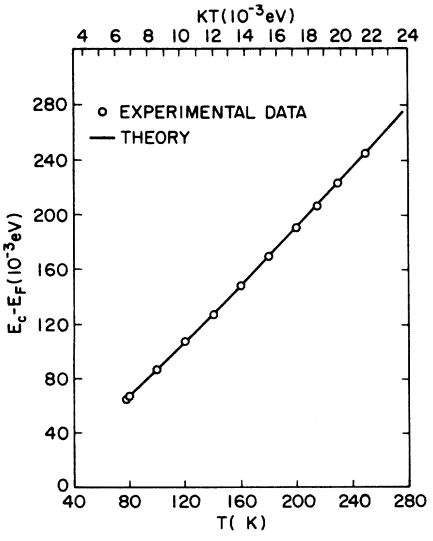

FIG. 8. Theoretical and experimental values of $E_c - E_F$ as a function of temperature.

IV. DISCUSSION

The temperature dependence of low-field, Hall-effect data taken between liquid nitrogen and room temperature on antimony-doped germanium is so strongly affected by changes in the correction factors that false decreases in carrier concentration are indicated (Fig. 3, upper curve). This low-field uncertainty, which prevents indentification of energy levels, is removed at high fields where straight-line plots of $\ln F$ vs $1/T$ have a slope determined by the depth of the ionizing donor level and an intercept determined by the density of states effective mass. Sufficient separation of the levels to provide clear discrimination between differing $\ln F$ vs $1/T$ straight lines (see Fig. 6) was found for levels differing by about a factor of 2 in distance from E_c. A good fit between theory and experiment was found for both the variation of n and of E_F with temperature.

The use of the high-field, Hall-effect technique developed in this study should prove most useful as a method for identifying the energy levels and densities of impurities in semiconductors that are deeper than the dominant, shallow level. At low B fields, changes in the Hall data due to ionization of deeper levels was obscured by the T variations of the correction factor AS. As temperature is raised, the ionization of deeper levels approaching the mid-gap region can be seen before band-to-band excitation begins to dominate as indicated by Eq. (12). Levels deeper than mid-band can be seen in materials that can be doped the opposite type (p type) since thermal excitation would then proceed from the opposite band edge (the valence-band edge) to the mid-band-gap regions.

The new criterion for ionization of an impurity level shown in Fig. 2 and Eq. (9) consistently explained why the energy levels identified in Fig. 6 were almost totally ionized at temperatures where KT was only a few tenths of the depth of the level from the band edge. The $\pm 0.2\%$ accuracy claimed for the high-field data is less than the difference

seen in Fig. 3 between the theoretical curve and the actual data points. The small deviations are of a form similar to that found when more than a single ground state of a donor is considered as discussed by Blakemore.[4] However, no significant improvement in fit was obtained by incorporating from one to six of Blakemore's excited states of the donors. This may mean that the slight differences (between the theory and experiment) are caused by splitting of the ground state in the crystal field such as found in phosphorous doped silicon[12] and discussed by Blakemore.[4] This was not included in the present analysis because any improved fit would have been as much as indication of the value of two additional fitting parameters as it would have been a verification of donor ground-state splitting. The maintenance of the same $1/T = 0$ intercept specified by the density of states effective mass as shown in Fig. 6 for the 77 to 273 K temperature range is an indication that the anisotropic effective masses originally determined at liquid helium temperatures by cyclotron resonance apply all the way up to room temperature.

ACKNOWLEDGMENTS

The $\ln F$ vs $1/T$ plotting technique described in this paper was initially developed as part of a thesis submitted by G. J. Sullivan to the faculty of the Electrical Engineering Department of the University of Delaware as partial fulfillment for the Master's of Electrical Engineering degree. The experimental part of this work was performed while authors L. D. Partain and M. R. Lakshminarayana were guest scientists at the Francis Bitter National Magnet Laboratory, which is supported at M.I.T. by the National Science Foundation. The authors wish to recognize the exceptional assistance of L. G. Rubin in obtaining the experimental data and for critically reading the manuscript. Very helpful discussions were held with J. J. Kramer on the theoretical interpretation of the experiments. The assistance of G. A. Armantrout in identifying known impurity levels in Ge is gratefully acknowledged. Significant changes were made in the manuscript in response to the very helpful comments of Robert S. Allgaier.

---

*Present address: Lawrence Livermore Laboratory, Livermore, California 94550.

†Present address: Electrical Engineering Dept., California State Polytechnic University, Pomona, California 91768.

‡Present address: Electrical Engineering Dept., University of California, Santa Barbara, California 93106.

[1]L. D. Partain and M. R. Lakshminarayana, J. Appl. Phys. 47, 1015 (1976).

[2]L. D. Partain, M. R. Lakshminarayana, and C. R. Westgate, J. Appl.Phys. 48, 2570 (1977).

[3]N. Cusack, *The Electrical and Magnetic Properties of Solids* (Wiley, New York, 1958), p. 209.

[4]J. S. Blakemore, *Semiconductor Statistics, International Series of Monographs on Semiconductors*, edited by H. K. Henisch (Pergamon, Oxford, 1962), Vol. 3, pp. 45, 142, 147.

[5]C. Kittel, *Thermal Physics* (Wiley, New York, 1969), p. 143.

[6]C. Herring, Phys. Rev. 96, 1163 (1954).

[7]E. M. Conwell, Proc. IRE 46, 1281 (1958).

[8]E. G. S. Paige, in *Progress in Semiconductors*, edited by A. F. Gibson and R. E. Burgess (Wiley, New York, 1964), Vol. 8.

[9]S. M. Sze and J. C. Irvin, Solid State Electron. 11, 599 (1968).

[10]T. H. Geballe and F. J. Morin, Phys. Rev. 95, 1085 (1954).

[11]Note the error in labeling the horizontal axis of Geballe and Morin's Fig. 1 (Ref. 10) which should read $100/T$.

[12]G. Picus, E. Burstein, and B. Henvis, J. Phys. Chem. Solids 1, 75 (1956).